Soil & Tillage Research 111 (2011) 197–207

Contents lists available at ScienceDirect

Soil & Tillage Research

journal homepage: www.elsevier.com/locate/still

Modeling edge effects of tillage erosion

Dalmo A.N. Vieira *, Seth M. Dabney [1]

USDA-ARS National Sedimentation Laboratory, P.O. Box 1157, 598 McElroy Drive, Oxford, MS 38655, USA

ARTICLE INFO

Article history:
Received 24 February 2010
Received in revised form 17 June 2010
Accepted 8 October 2010

Keywords:
Tillage erosion
Tillage translocation
Tillage berms
Field boundary
Morphological feature
Mathematical models
Vegetative barriers
Lynchets
Bench terraces
Landscape evolution

ABSTRACT

Tillage erosion has been recognized as an important factor in redistribution of soil over time and in the development of morphological changes within agricultural fields. Field borders, fences, and vegetated strips that interrupt soil fluxes lead to the creation of topographic discontinuities or lynchets. When tillage tools that preferentially throw soil to one side are used repeatedly to move soil in one direction, rather than alternating with each pass, they create berms at the receiving side of the tilled domain and a "dead furrow" or channel at the contributing side. However, even tillage implements that are symmetrical in throwing soil equally in both lateral directions on flat surfaces may throw some soil beyond the implement width and so contribute to soil berms formation just beyond the tilled zone that can affect water flow paths. We developed a two-dimensional Tillage Erosion and Landscape Evolution Model that allows complex internal boundaries to be defined within the simulation domain. In this paper we develop and demonstrate techniques and tools to allow prediction of the formation of edge-of-field berms by defining alternative boundary conditions. The derivation and assumptions of the model are presented and then it is applied and compared to survey results from two field studies: one an experimental field in Coffeeville, Mississippi, where grass hedges were planted close to field elevation contours to evaluate their effectiveness as an erosion control measure and were monitored over a 16-year period; and the other a set of 0.1 ha plots located near Holly Springs, MS where the effect of edge-of-field berm formation on runoff partitioning was evaluated during an 8-year study. Results demonstrate the ability of the model to correctly reproduce the location and magnitude of soil loss and accumulation. At Coffeeville, erosion averaging over 20 cm in the downslope side of each grass hedge and deposition taking place near the slope ends led to the formation of lynchets up to 0.8 m high, and the average slope steepness in the cropped areas between hedges decreased from an average of 7.2% in 1993 to about 3.7% in 2009. In Holly Springs, repeated tillage conducted next to grass hedges planted along the hillslope bottoms led to the formation of berms with average height of 13 cm, which may significantly alter field-scale hydrological, erosion, and sediment transport processes.

Published by Elsevier B.V.

1. Introduction

Tillage erosion has been reported to significantly contribute to the modification of agricultural landscapes, and it has been extensively documented (Lindstrom et al., 1992; Lobb et al., 1995; Govers et al., 1996; Van Oost et al., 2000; Li et al., 2009). Tillage implements displace soil at rates that vary according to the terrain steepness and operational factors, including: implement type and size; tillage depth, speed, and orientation relative to the slope; and soil condition before tillage. Net soil loss or accumulation occurs when soil translocation rates change relative to adjacent areas. In complex landscapes, tillage erosion usually occurs near convexities, such as hilltops and knolls, and on upslope field areas, while deposition occurs at concave slope positions and at hill bottoms. The presence of any feature that interrupts or modifies the soil movement by tillage may lead to increased local rates of erosion and/or deposition. Field borders, vegetative barriers, fences, and terrace berms are examples of features that commonly induce localized morphological changes.

The effects of tillage erosion are often evident in the upper part of hillslopes, locations where water erosion is less intensive (Lindstrom et al., 1990). Repeated tillage operations can lead to exposure of subsoil, which can be detrimental to agricultural production (Schumacher et al., 1999). While not recognizing tillage erosion as a separate process, Lowdermilk (1953) described how farmers in southern France, periodically excavated the lower furrows, transported the soil uphill, and spread it along the degraded upper edge of the field.

"Lynchet" is an archeological term referring to the morphological response on a hillslope to the presence of field boundaries in

* Corresponding author. Tel.: +1 662 232 2951; fax: +1 662 281 5706.
E-mail addresses: dalmo.vieira@ars.usda.gov (Dalmo A.N. Vieira), seth.dabney@ars.usda.gov (S.M. Dabney).
[1] Tel.: +1 662 232 2975; fax: +1 662 281 5706.

0167-1987/$ – see front matter. Published by Elsevier B.V.
doi:10.1016/j.still.2010.10.007

Nomenclature

CV	Control volume
f_b	Mass transfer factor between field and berm
f_P, f_R	Mass transfer factors of a permeable boundary
h_B	Maximum field berm height
h_b	Field berm height (current value)
i, j	Grid number along x and y directions
$\vec{n}$	Unit vector normal to a cell face
P	Computational node at the center of a control volume
w_B	Initial field berm width
w_b	Field berm width (current value)
x	Cartesian direction or axis
y	Cartesian direction or axis
z	Cartesian direction or axis; Terrain elevation
α	Soil translocation amount for level land ($kg\,m^{-1}\,pass^{-1}$)
α_B	Soil translocation amount toward field berm ($kg\,m^{-1}\,pass^{-1}$)
β	Soil translocation coefficient related to slope gradient ($kg\,m^{-1}\,\%^{-1}\,pass^{-1}$)
$\Delta x, \Delta y$	Cell sizes in the x and y directions
Φ	Soil mass flux in units of mass per tillage operation
ϕ	Soil mass flow rate per unit width per tillage operation
ϕ_B	Soil mass flow rate at the cell face opposite to a boundary
ϕ_b	Soil mass flow rate at the cell face that defines a boundary
φ_1	Field berm side slope (inner side)
φ_2	Field berm side slope (outer side)
ρ_b	Soil bulk density

Subscript

E	Computational node to the East
e	East face of a control volume
N	Computational node to the North
n	North face of a control volume (subscript); time integration level (superscript)
S	Terrain slope gradient in percentage; computational node to the South
s	South face of a control volume
W	Computational node to the West (subscript)
w	West face of a control volume (subscript)
1	Refers to tillage direction (subscript)
2	Refers to direction perpendicular to tillage direction (subscript)

cultivated landscapes (Bell, 1992). Lynchets dating from Bronze Age, Iron Age, and medieval periods have been observed to form at all cultivated field boundaries whether bounded by untilled grass strips, fences, or ditches. While medieval lynchets tend to be oriented along the slope, older "Celtic fields" are often square, retain cross-plowing tillage marks, and are bounded by lynchets on all sides (Fowler and Evans, 1967). Some lynchets are oriented obliquely up and down the slope (Smith, 1975). The accelerated formation of lynchets in contemporary times has been observed around the world (e.g. Papendick and Miller, 1977; Lewis, 1992; Dabney et al., 1999; Turkelboom et al., 1999; Dercon et al., 2007). Jacobson (1963) described how bench terraces could be engineered to develop gradually through planned and controlled tillage translocation.

Tillage performed parallel to field borders often creates narrow areas of deposition in the untilled area alongside the border. With time, deposited soil clods coalesce to form a small berm with an associated channel at the edge of the field (Dabney, 2006), as shown in Fig. 1. These edge-of-field berms may affect the rate and the distribution of runoff from the fields, as they may create temporary impoundments. Water flows concentrated in these channels may follow a buffer edge until a low point is reached where the berm will be overtopped. This may be considered desirable or undesirable. For example, berms may prevent runoff from entering a grass waterway, causing it to erode areas to the side of the waterway. The conservation practice standard for "contour buffer strips" (USDA-NRCS, 2007) states that if "sediment accumulates just below the upslope edge of the buffer strip to a depth of 6 inches or more ... relocate the buffer/cropped strip interface location." In contrast, vegetative barriers (USDA-NRCS, 2003) may be designed to divert runoff by deliberately allowing berms to develop. Tillage berms may occur also in the middle of a field, especially for one-way implements such as a moldboard plow, and their characteristics depend on the type of implement, tillage pattern, and superposition of sequential tillage passes (Li et al., 2009).

In this study, the formation and evolution of morphological features created by tillage erosion at field boundaries and along vegetative buffers were investigated. The Tillage Erosion and Landscape Evolution Model (Vieira and Dabney, 2009) was used to simulate morphological changes caused by repeated tillage operations between untilled vegetative barriers, and the development of edge-of-field berms at the boundary between tilled and vegetated areas. Model predictions were assessed through comparison with field observations for sites in North Mississippi.

2. Tillage Erosion and Landscape Evolution Model

2.1. Model description

Vieira and Dabney (2009) described the Tillage Erosion and Landscape Evolution Model (TELEM) that computes erosion and deposition resulting from soil translocation created by tillage implements using the scheme illustrated in Fig. 2. TELEM allows for the presence of complex field boundaries and uses actual tillage patterns and local terrain steepness to determine soil translocations over the terrain using a Finite Volume Method (FVM) solution of the soil mass balance equation at computational nodes located at the centers of the non-overlapping control volumes (*CV*s).

In the model, soil translocation is computed for each node using empirical relations proposed by Lobb and Kachanoski (1999). Soil movement is determined independently for the direction of tillage and the direction perpendicular to it:

$$\phi_1 = \alpha_1 + \beta_1 S_1, \tag{1a}$$

$$\phi_2 = \alpha_2 + \beta_2 S_2, \tag{1b}$$

where ϕ_1 is the mass flow rate in kilograms per meter width per tillage pass. The coefficient α_1 is the net translocation amount in the tillage direction on level ground; β_1 is the slope steepness coefficient, characteristic of the tillage implement; and S_1 is the slope gradient (%) in the tillage direction. Similarly, Eq. (1b) refers to soil movement in the lateral direction, identified by the subscript 2. This approach means that the soil mass flow rate at the

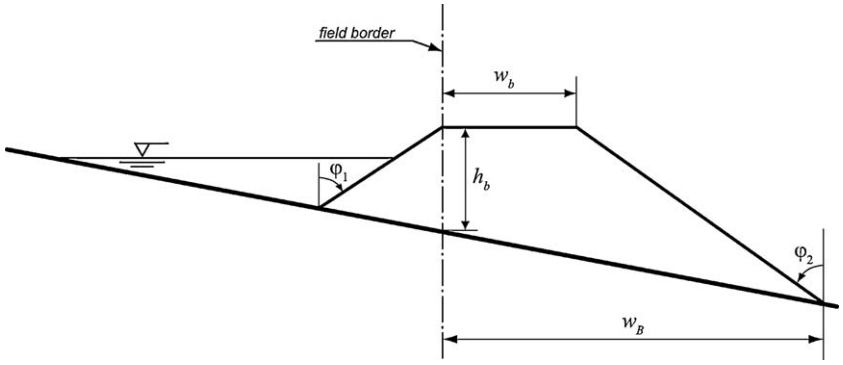

Fig. 1. Edge-of-field berm and channel. Berms can create temporary impoundments and concentrate and divert runoff to a point where the berm is breached or overtopped. In the model, the idealized berm geometry is defined by the initial width w_B and the angles φ_1 and φ_2; with each tillage pass, the berm height h_b increases while the berm's top width w_b decreases.

center of a cell is represented by a vector $\vec{\phi}$, whose components are the soil translocation rates ϕ_1 and ϕ_2. This same quantity can be expressed as components normal to the cell faces ϕ_x and ϕ_y, as illustrated in Fig. 2b. These translocation relations were selected because they enable the simulation of repeated operations in the same direction, which can be particularly important near field boundaries. An extensive data base of α and β coefficients is available and continues to expand (Lobb et al., 1995, 1999; Van Muysen et al., 2000, 2002, 2006; Van Muysen and Govers, 2002; Da Silva et al., 2004; Heckrath et al., 2006; Tiessen et al., 2007a,b,c, 2009; Li et al., 2007a,b). Vieira and Dabney (2009) provide a detailed derivation of the model, present a number of verification tests, and discuss the choices for equations and methods, the impact of the selection of mesh sizes on the numerical solutions, and the model's advantages and limitations.

2.2. Input data processing

Geographical Information Systems (GIS) provide a practical framework to support the modeling of actual fields using the two-dimensional cell-based tillage erosion model. Terrain elevations are specified in the form of digital elevation models (DEMs) created at the spatial resolution used in the simulations. Field boundaries, such as field borders, vegetative barriers, and fences are described by GIS lines and polygons. Tillage directions are prescribed as line segments describing the trajectories taken by the tillage implements over the field. User-given path lines are then converted into tillage directions for each computational cell, thus allowing the approximation of actual, curvilinear tillage paths. TELEM pre-processes these GIS layers to determine which DEM cells belong to the computational domain and to define how boundary conditions are applied to the corresponding cell faces. TELEM requires that field boundaries coincide with the location of the *CV* faces, but boundary conditions can be applied separately to each face. The possibility of representing in the mathematical model diverse situations observed in agricultural fields invites a more careful analysis of methods available for the treatment of field boundaries.

3. Generalized boundary types

Tillage erosion models developed in the past disregarded the direct effects of physical boundaries on the process of erosion, limiting the analysis to interior areas, or employed simplified boundary conditions that may not reflect realistically the conditions observed during real tillage operations in agricultural fields (e.g. Lindstrom et al., 2000; Van Oost et al., 2000; De Alba, 2003; Li et al., 2007a, 2009). In order to predict morphological changes induced by the presence of physical barriers, TELEM implements three types of boundary conditions which describe how the presence of a physical boundary affects local soil displacement and triggers localized soil erosion or deposition.

A "closed" boundary condition, perhaps the most evident type, enforces the situation where no soil traverses the face where the condition is applied. This is the type used for high field berms or

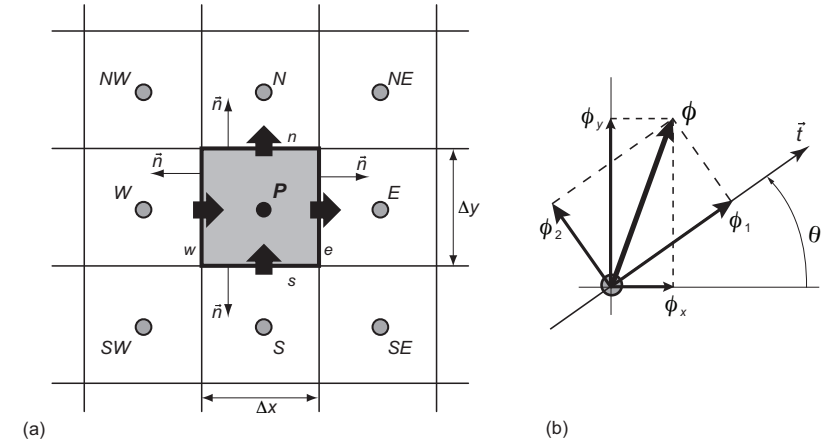

Fig. 2. (a) Two-dimensional grid and control volume. Each *CV* has a central node *P*, where properties are computed; neighboring cells are referred to by the cardinal points (*E*, *W*, *N*, *S*), and the *CV* surface is represented by four planar faces (*e*, *w*, *n*, *s*), parallel to the Cartesian directions. (b) Tillage translocation vectors. The total net translocation vector ϕ is the sum of its components ϕ_1 and ϕ_2, computed in the direction of tillage ($\vec{t}$) and perpendicular to it, respectively. The same vector can be represented by components normal to the cell faces (ϕ_x and ϕ_y) representing soil fluxes from and into neighboring cells, from which elevation changes for the cell are computed using a mass balance equation (after Vieira and Dabney, 2009).

very dense or impenetrable vegetative barriers, for example, where it can be assumed that the amount of soil that traverses boundary is negligible. Numerically, it consists of simply setting the flux across the corresponding faces of all *CV*s along the boundary to zero ($\phi_{\vec{n}} = 0$). This type of boundary condition leads to either deposition or erosion in the computational cell where it is applied, depending on the direction of the component of the soil flux normal to the boundary. If the soil is moving away from the boundary, soil loss occurs, otherwise accumulation occurs.

An "open" boundary condition allows the soil to cross the *CV* face at a rate and direction equal to the rate computed for the opposite face of the same *CV* ($\partial\phi/\partial\vec{n} = 0$). This type of condition is useful when simulating an "open-ended" domain, where no physical boundary exists. Practical applications of this type of boundary condition include situations where tillage extends beyond the model boundaries, or when the exact location where tillage starts and stops is unknown. It can also be used when tillage boundaries vary between operations. This condition is useful because it does not let the presence of the boundary influence the soil movement inside the simulated region. There is no localized erosion or deposition near the boundaries when this condition is used. Soil flows out of the simulation domain if the computed soil flux is toward the boundary. Conversely, soil enters the field if the computed soil flux is directed away from the boundary.

"Permeable boundaries" allow soil to move through with a rate that is proportional to the soil translocation perpendicular to the boundary, computed at the boundary cell. It is a way to simulate a boundary response to soil displacements taking place in their vicinity. Soil is allowed to cross the boundary only if certain conditions are met. This situation is represented in the model by making the soil mass flux across the boundary a function of the soil flux across the opposite face of the boundary cell, or:

$$\phi_b = \begin{cases} f_P\phi_B & \text{if } (\vec{\phi}\cdot\vec{n}) > 0, \\ f_R\phi_B & \text{if } (\vec{\phi}\cdot\vec{n}) < 0, \end{cases} \quad (2)$$

where ϕ_b is the mass flux at the boundary face, ϕ_B is the flux entering the boundary cell (normal to the boundary), and f_P and f_R are boundary permeability factors, which are applied separately, depending if the soil flux is toward or away from the boundary. Note that the boundary condition represented by Eq. (2) reduces to the "closed" boundary condition when $f_P = f_R = 0$ and to "open" boundary when $f_P = f_R = 1$.

4. Modeling the development of field berms

In the model, special boundary cells are used to describe the geometry of tillage berms at scales smaller than the mesh size, assuming that field berms develop with a trapezoidal geometry as shown in Fig. 1. Soil is initially distributed over a distance w_B beyond the field boundary, defining the initial berm width. As the berm develops, less soil leaves the field, soil is distributed over a smaller width, and part of the soil is reflected by the berm and deposited in the field next to the berm, leading to the trapezoidal shape. The side slopes of the berm reflect how soil displacement is reduced when the berm height increases.

The model calculates the rate at which soil is moved into the berm as a function of both soil translocation toward the boundary and current berm height. The soil flux crossing the boundary is determined by

$$\phi_b = f_b\phi_B \quad (3)$$

and

$$f_b = f_P\left(1 - \frac{h_b}{h_B}\right), \quad (4)$$

where f_b is a factor that determines the mass transfer rate from the field to the berm. This factor is adjusted according to the berm height h_b measured at the boundary, and varies from its maximum value f_P to zero when the maximum height h_B is reached. The part of the soil that is thrown toward the berm but returns to the field and is deposited just next to the berm is:

$$\phi_r = (1 - f_b)\phi_B. \quad (5)$$

The berm geometry is adjusted after each tillage pass. The increment in berm height is determined from the berm geometry and soil flux toward the berm ϕ_b:

$$\Delta z_b = \frac{w_b - \sqrt{w_b^2 - 2\tan\varphi_2\phi_b/\rho_b}}{\tan\varphi_2}. \quad (6)$$

The berm height is $h_b^{n+1} = h_b^n + \Delta z_b$, and the new berm width is $w_b^{n+1} = w_b^n - \Delta z_b\tan\varphi_2$, where the superscript n indicates a tillage pass. Soil that returns to the field, computed with Eq. (5), is distributed to form the inner slope of the berm, according to the slope angle φ_1. Any excess return soil is redistributed within the boundary cell. If for a tillage pass, the computed soil flux toward the berm causes the maximum berm height to be surpassed, the flux ϕ_b is limited so that only the mass of soil necessary to make the berm reach its maximum is actually transferred to the berm.

The parameters h_B, w_B, φ_1 and φ_2 define the berm's geometry and can be deduced from field observations. The parameter h_B is a function to implement type and size; w_B relates to the distance soil is thrown in the lateral direction, and therefore it is associated with implement size and design, tillage speed, and the presence of vegetation in the field border. The factor f_P in Eq. (2) reflects the vegetation density at the field boundary, but it also relates to tillage tool's setup and adjustment, as it describes the non-uniformity of the net lateral translocation, allowing the specification of a smaller translocation near the implement's extremities (Fig. 3c).

Symmetrical implements such as tandem disks are designed to balance lateral soil displacement created by disk gangs, resulting in negligible net displacement when operating on level ground ($\alpha_2 \cong 0$). Notwithstanding these design measures, it is frequently observed that soil is thrown beyond the implement width, as shown in Fig. 3a, forming ridges that are removed when tillage passes overlap, but that remain next to field borders. In the model, the amount of soil translocated beyond the implement width is accounted for by an additional parameter α_B (kg m^{-1} pass^{-1}), used only for boundary cells. Therefore, the soil flux toward the berm is computed as $\phi_B = \max(\phi_B, \alpha_B)$ so that the localized deposition at the field border is always considered.

5. Field observations and simulation of edge-of-field berm formation

5.1. Field description

Four 0.1 ha plots at the North Mississippi Branch of the Mississippi Agricultural and Forestry Experiment Station near Holly Springs in Marshall County, Mississippi, were used to investigate the performance of vegetative barriers as an edge-of-field soil conservation practice. The plots, measuring 45.7 m × 22.1 m, were built with a 5% grade along the smaller dimension, and 0.3% grade in the longest direction (Mutchler et al., 1994). Soils in the plots were Providence silt loam (fine-silty, mixed, active, thermic Oxyaquic Fragiudalfs; Fragic Luvisols in the FAO classification) and Memphis silt loam (fine-silty, mixed, active, thermic Typic Hapludalfs; Haplic Luvisols). A concrete-lined channel was built along the bottom of the 5% slope. In two of the plots (N5 and E5), a switchgrass (*Panicum virgatum* L.) grass

Fig. 3. (a) Soil being displaced laterally, beyond implement width. Soil accumulation from repeated tillage operations can lead to the formation of berms that flank the field. (b) Soil displacement created by disk gangs. Small imbalances in lateral translocation created by the implement design or adjustment can create ridges or furrows near the implement's ends; rear gangs are often wider than the front gangs to minimize soil displacement beyond the implement width. (c) Tapered disk blades are used to improve soil distribution and leveling.

hedge about 1.0 m wide was seeded parallel and just upslope of the concrete channel, as shown in Fig. 4a. The hedge was established in 1996, and the field was planted to corn (*Zea mays* L.) between 1996 and 2004. The remaining plots (S5 and W5) were built and managed in a similar manner, but did not have the vegetative barrier at the bottom of the slope.

Tillage operations were conducted every spring between 1996 and 2004, and consisted of one pass of a chisel plow, two passes of a

Fig. 4. (a) Grass hedge and concrete channel at the downslope end of plot N5. (b) Detail of the field berm next to the grass hedge.

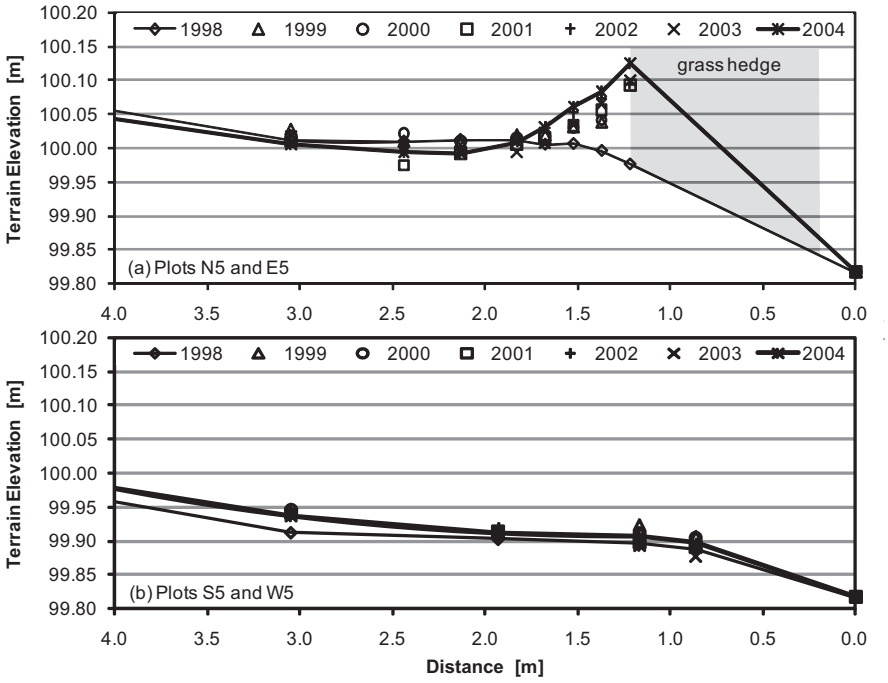

Fig. 5. Average hillslope profiles for plots: (a) with vegetative barriers (N5 and E5); and (b) without vegetative barriers (S5 and W5), measured between 1998 and 2004. Solid lines emphasize the morphological changes observed for the two sets of plots, where tillage berms developed only for plots with vegetative barriers.

tandem disk, and one pass of a do-all (combination of a reel pulverizer and a finishing harrow). Tillage implements were taken along paths parallel to the longest plot dimension, and always conducted in the same direction, with the tractor entering the field from the side away from the flume. Starting from 2001, tillage was performed with the explicit instruction that the implement be driven very close to the grass hedge, whereas in earlier years care was taken to chisel and disk at some distance from the boundary so that the do-all finishing harrow could smooth any berm created.

Topographic surveys were conducted for all plots along three transects, at distances of 7.6 m, 22.9 m, and 38.1 m, measured along the concrete channel from the lower corner of the plot. Surveys were taken biannually, before the spring tillage and again in the fall. Between 1996 and 1998, elevation surveys were limited to 3.0 m above the concrete; after that, surveys extended to cover the entire slope. Survey data indicated a consistent 5% slope toward the hillslope bottom, with an area of tillage-induced deposition at the end of every plot. Initially, a flat area developed between 1996 and 1998. Berms started to form on the plots with hedges when tillage was moved adjacent to the grass strips. For the plots with vegetative barriers, the berms grew with their crests approximately aligning with the edge of the vegetation, as shown in Fig. 4b. The geometry and size of the berms in the two plots were essentially similar, reaching average heights of 0.16 m (0.17 m maximum) for the plot E5, and 0.12 m (0.14 m maximum) for plot N5.

Elevation data from the plots were averaged to create representations of the hillslope and berm profiles for each date surveys were taken. Fig. 5 shows profiles for the plots with and without grass hedges, where the lines highlight the profiles at the beginning and end of the survey period. For plots with grass hedges, berms developed and persisted, while for the plots without vegetation, berms are not evident.

5.2. Modeling field berm development

The average profile for plots E5 and N5 determined from the topographical survey of March 1998 was used as the initial topography for the model simulation. A computational mesh with resolution of 0.5 m was created, with the boundary of the tillage domain coinciding with the upslope edge of the grass hedge. The model was used to compute berm development and morphological changes in the vicinity of the grass hedges for the period between 1998 and 2004.

Tillage translocation coefficients for each implement (Table 1) were chosen based on values available in the literature (Lobb et al., 1999; Tiessen et al., 2007a,b, 2009). There is some degree of uncertainty in the choice of these coefficients, particularly for lateral translocation caused by tillage on the contour with symmetrical implements such as disks or chisel plows. For all implements, it was assumed that the rate of lateral soil translocation on level ground α_2 was zero. Soil translocation rates toward the berm (α_B) were chosen based on the evolution of berm heights observed in the Holly Springs plots. A soil bulk density of 1500 kg m^{-3} was assumed.

At the grass hedge, a berm-type permeable boundary condition was specified. It was assumed a maximum soil transfer factor between the field and the berm $f_P = 0.6$, which accounts for the fact

Table 1
Tillage translocation coefficients used in the simulations of berm development in Holly Springs, and of terrace bench development in Coffeeville.

Implement	α_1 (kg m^{-1} pass^{-1})	β_1 (kg m^{-1} %$^{-1}$ pass^{-1})	α_2 (kg m^{-1} pass^{-1})	β_2 (kg m^{-1} %$^{-1}$ pass^{-1})	α_B (kg m^{-1} pass^{-1})[a]
Chisel Plow	60.0	1.8	0.0	0.9	3.5
Tandem Disk	50.0	2.0	0.0	1.0	5.0
Do-All	20.0	0.7	0.0	0.35	0.5

[a] Berm translocation coefficient α_B taken = 0 for the Coffeeville field.

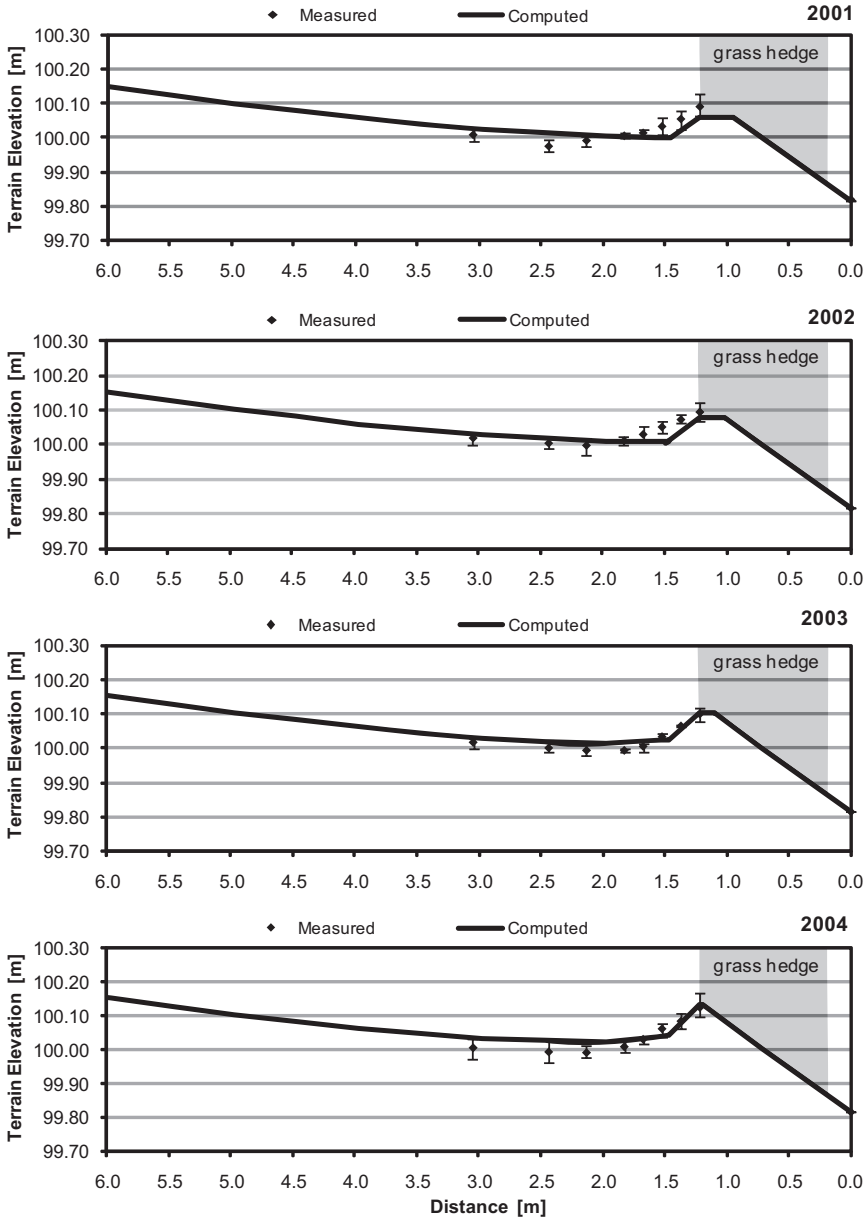

Fig. 6. Development of edge-of-field berm. Measured and simulated profiles for plots in Holly Springs, Mississippi. Lines indicate model simulation; symbols indicate averaged surveyed elevations and error bars show the range of deviations from the average elevation.

that the vegetation reduces transfer of soil to the area where the berm is forming. Soil launched into the vegetated area is assumed to be initially thrown over a distance of 0.5 m beyond the implement width, which approximately matches the berm dimensions observed in the field. The berm side slopes were set to 15° from the horizontal ($\varphi_1 = \varphi_2 = 75\ ^\circ$).

Comparison of measured and computed profiles (Fig. 6) showed the model was able to reproduce the process of localized deposition by tillage, and formation of the edge-of-field berms. Simulation results showed a continuous increase of the berm height, accompanied by the gradual development of an adverse slope above the grass hedge due to deposition next to the berm. As the berm developed, its crest width decreased, and the trapezoidal cross section evolved into a triangular shape. Generally, model predictions were similar to elevation changes observed in the field measurements. The model predicted deposition at the transition of slope steepness (approximately 3.0 m above the concrete channel), resulting from the change in soil translocation. It also showed deposition in the flat area next to the berm. General agreement between the computed and the observed average berm profiles for each year can be assessed using the Nash–Sutcliffe efficiency (Nash and Sutcliffe, 1970), defined as $NSE = 1 - \sum_{i=1}^{n} (z_o^i - z_m^i)^2 / \sum_{i=1}^{n} (z_o^i - \bar{z}_o)^2$, where z_o^i and z_m^i are the observed and modeled terrain elevations, $\bar{z}_o$ is the mean of the observed data, and n is the number of observations. An efficiency of $NSE = 1$ corresponds to a perfect match between modeled and observed data. *NSE* values computed for the years 2001–2004 are 0.45, 0.46, 0.82 and 0.76, respectively, indicating that the observed berms grew quickly, while their development in the model was more gradual.

6. Field observations and simulation of the development of bench terraces

6.1. Field description

In an experimental field near Coffeeville, Yalobusha County, Mississippi, vegetative barriers were planted close to field

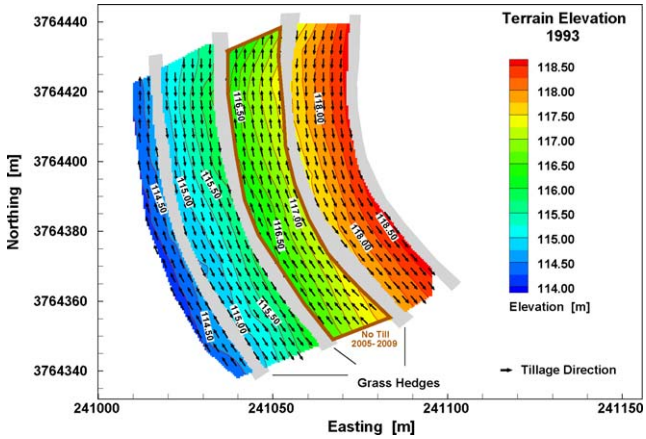

Fig. 7. Test field near Coffeeville, Mississippi. Colors indicate topography, and gray areas indicate the location of vegetative barriers. Area indicated in the center of the field was cropped with no-till techniques after 2005. Arrows indicate the directions of the first tillage pass; directions are reversed after each pass.

elevation contours to evaluate their effectiveness as an erosion control measure and to investigate the formation of landscape benching (Dabney et al., 1999). Three parallel hedges 1.5 m wide were established on the contour, spaced about 20 m apart, across a fairly uniform 6.8% slope. The field was located on Loring silt loam (fine-silty, mixed, thermic, active, Oxyaquic Fragiudalfs; Fragic Luvisols). The grass hedges were planted during the summer and autumn of 1992. A topographic survey was conducted in July 1993, and immediately after, a tillage fallow management began, which lasted until 2001, when winter cover crops were established. Starting in 2003, the field was double cropped to soybean (*Glycine max* L.) and wheat (*Triticum aestivum* L.), and rotated with corn after 2005. Fig. 7 shows the test field, the location of the grass hedges, the 1993 topography, and the initial tillage directions.

Tillage passes were performed parallel to the grass hedges, following the same curvilinear path, using an offset tandem disk, a chisel plow, and a do-all, for a total of 126 tillage passes, conducted between the Spring of 1993 and the Fall of 2007. During the first three years, a tractor-pulled rototiller was used in the 1.2 m upslope of the hedges. All operations were performed with two passes, with tillage directions being reversed after each pass, and with the specific instruction that the passes next to the grass hedges be conducted at reduced speed to avoid throwing soil into the vegetation. Starting in 2005, an area in the center of the field, indicated in Fig. 7, was cropped with no-till techniques.

6.2. Simulation of the development of bench terraces

The tillage erosion model was used to compute landscape evolution and the formation of bench terraces during the period 1993–2009. A DEM with 0.5 m resolution was created from the 1993 topographic survey (Dabney et al., 1993). The tillage area, used to define the extent of the simulation domain, was obtained from an aerial photograph taken in the winter of 1995, and the exact location of the hedges was obtained from a GPS-based survey taken in 2005. After automatic processing of the boundary data, the simulation domain contained 18,460 active cells, 1517 of them adjacent to a hedge or field boundary.

Sensitivity analysis showed that the morphological change created by contour tillage near field boundaries was not particularly sensitive to the choice of the cell size of the computational mesh for sizes between 0.5 and 5.0 m (Vieira and Dabney, 2009). In the current application, a mesh size of 0.5 m was chosen because the small sizes better represented the curved grass hedges.

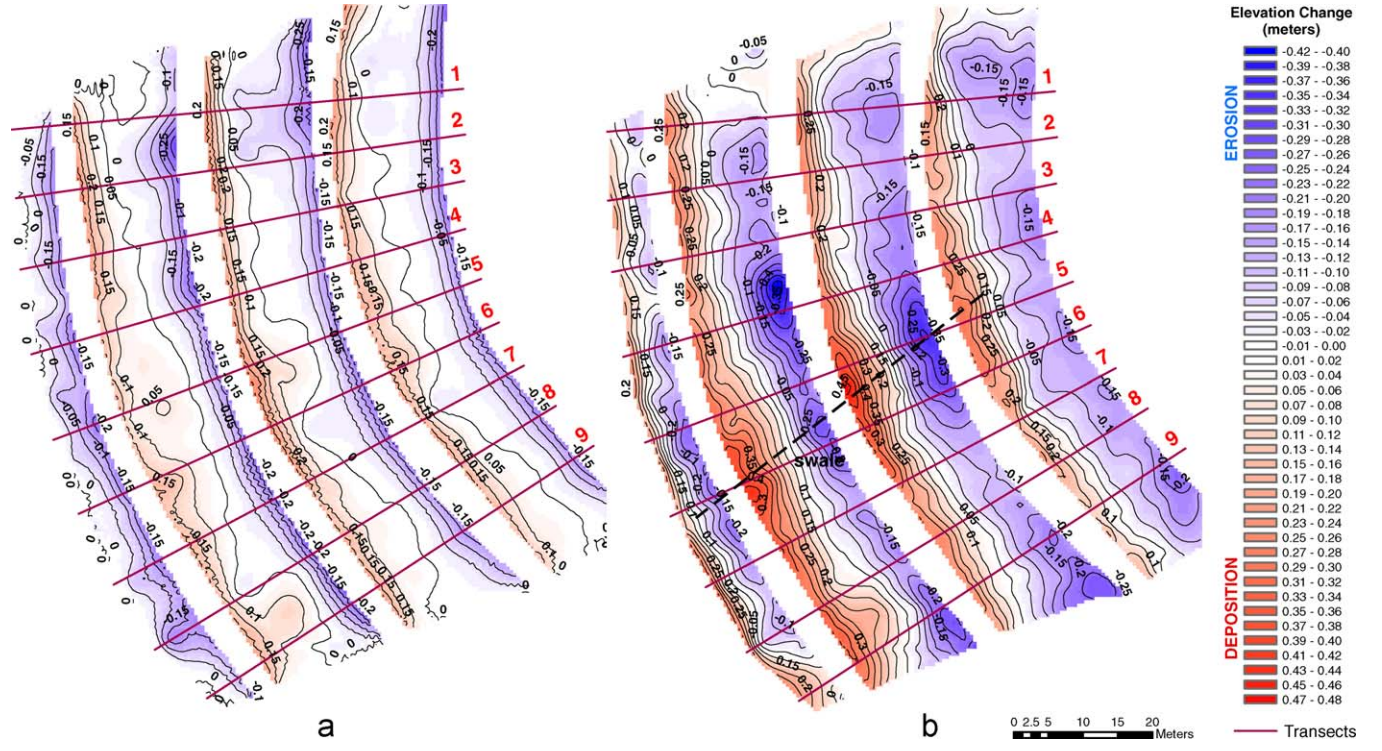

Fig. 8. Computed (a) and measured (b) erosion and deposition, between 1993 and 2009, assuming "closed" boundaries at the grass hedges. Erosion (negative values, shown in shades of blue) occurred downslope of the grass hedges while deposition (positive values, shades of red) occurred above the hedges. Purple lines numbered 1–9 identify cross sectional profiles.

The tillage operations were converted into an XML input file describing 43 tillage events, some of which involved more than one implement on the same day. The few rototiller operations, limited to a narrow band near the hedges, were not included in the simulations. The curvilinear tillage paths were described by specifying a different tillage direction for each computational cell. Each tillage implement was characterized by soil translocation coefficients, summarized in Table 1. The lateral soil translocation coefficient α_2 is zero for symmetrical implements, and the soil translocation rate toward the berm (α_B) is also taken as zero because care was taken so that soil was not thrown toward the vegetation; the coefficient β_2 determines the rate of soil translocation and development of bench terraces. Bulk density was measured in 1997 at several locations in the test field. The average value of 1380 kg m^{-3} (Dabney et al., 1999) was used in the simulation. For the generally east and west cell faces adjacent to hedges, the "closed" boundary condition was used. The "open" condition was applied to the field limits in between hedges at the North and South sides.

Fig. 8a shows the computed accumulated erosion and deposition amounts between 1993 and 2009. The figure shows a pattern of erosion downslope of each grass hedge, and deposition in the upslope side. Tillage operations also caused original depressions to be filled, and knolls to be eroded. The mid-slope portions between grass hedges do not show significant elevation differences, but local steepness decreased from the initial 7–8% in 1993 to about 5% in 2009. The average slope steepness in the cropped areas between grass hedges decreased from an average of 7.2% in 1993 to about 3.7% in 2009, reflecting the additional flattening that occurred in the proximity of the hedges.

Fig. 8b shows the net elevation changes the same period, computed as elevation differences using DEMs for the 1993 and 2009 field surveys. This map reflects both tillage and water erosion and deposition. The largest amounts of erosion and deposition are found near the center of field, where a swale in the initial topography crossed all three hedges and concentrated runoff water and sediment.

Fig. 9 shows measured and computed erosion and deposition for three of the transects indicated in Fig. 8. Profiles were extracted from 0.5-m DEMs created for both measured and computed data. The figure illustrates clearly the formation of boundary lynchets at the location of the vegetative barriers. Morphological changes computed by TELEM more closely matched observed erosion and deposition patterns at the north and south ends of the field. In the middle of the field, large discrepancies are seen where water erosion and deposition were increased by the presence of the

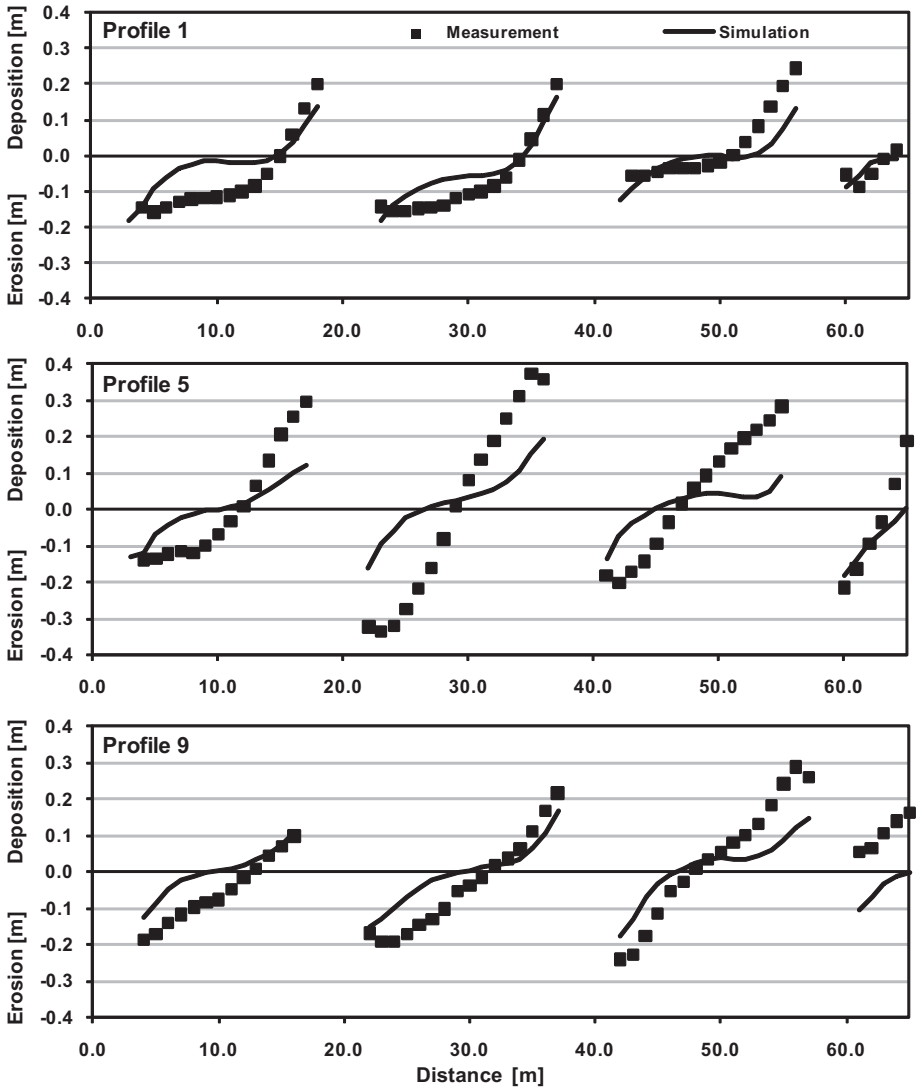

Fig. 9. Measured and computed erosion and deposition in the Coffeeville field between 1993 and 2009 for cross-sectional profiles 1, 5, and 9.

Table 2
Nash–Sutcliffe efficiencies (NSEs) and root mean square errors (RMSEs) evaluated for selected profiles of the Coffeeville field.

Profile	1	2	3	4	5	6	7	8	9	Overall
NSE	0.65	0.73	0.61	0.50	0.51	0.62	0.64	0.51	0.60	0.56
RMSE	0.06	0.06	0.07	0.11	0.13	0.11	0.08	0.08	0.09	0.09

swale. Table 2 presents root mean square errors (RMSE) and Nash–Sutcliffe coefficients computed for each of the profiles shown in Fig. 8. Because the measured topography embodies the effects of both tillage and water erosion, the indices are not necessarily indicators of the model's performance, but instead reflect the relative importance of water erosion. Smaller NSE and larger RMSE for the profiles in the middle of the field (profiles 4–6) indicate a larger contribution of water erosion.

7. Discussion

7.1. Permeable boundaries

Several practical applications exist for TELEM's permeable boundary type. Vegetation density is a factor that determines how much soil permeates the vegetation bordering a tilled field. Soil displaced by tillage is often moved into vegetated areas because the vegetation cannot block completely the soil that is pushed or thrown by tillage implements. The amount of soil that enters the vegetated area can be assumed to be proportional to the local soil translocation and the properties of the vegetation that restrict soil translocation. The factor f_P (Eq. (2)) dictates how much sediment can cross the boundary into the vegetated area: a larger f_P would represent a more permeable boundary, indicating a certain type or level of maturity of the vegetation.

An alternative conception of a permeable boundary condition is uncertainty in the location of the tillage boundary. Because field edges often vary from pass to pass, some soil is lost from the field, and in other occasions, soil is brought back from surrounding areas. This variability can be simply due to lack of precision, or it can be intentional, executed to curb vegetation growth that threatens to invade the cultivated field, or to eliminate berms that commonly form along field borders. The factor f_P controls the amount of soil lost from the tilled field through the boundary, while the factor f_R is used as a soil recovery factor for instances when tillage intrude neighboring areas and soil is returned to the field. The boundary in the model represents an average location of the field boundary, which may vary slightly from year to year but cancel out in the long-term.

A third application of permeable boundaries is when tillage occurs along fences or ditches. Fences enforce a linear boundary whose position cannot be exceeded. It does not necessarily stop soil from crossing it, but once crossed, soil cannot return. A ditch bordering a tilled field could be modeled in the same manner. These features require a boundary condition that allows soil movement in a single direction. The same condition described by Eq. (2) can be used if the factor f_R is set to zero. The factor f_P specifies the amount of soil that passes through the fence or falls in a ditch.

7.2. Tillage berms

In this study, we monitored the rapid development of tillage berms next to grass hedges in two plots in Holly Springs, but berms were not observed at Coffeeville. Several reasons may have contributed to the formation and continued reinforcement of tillage berms in one field and not in the other.

The details of the design and adjustments of tillage tools affect how soil is displaced to the sides, and determine how much soil is thrown beyond the implement width and control if berms or dead furrows form at field boundaries. Soil thrown beyond the width of an implement on level ground (Fig. 3a) creates an area of deposition that can develop into a berm after repeated passes. Some symmetrical implements, such as tandem disks, can be interpreted as two successive passes of unidirectional implements with translocation directions reversing with each pass (Fig. 3b). These tools are usually designed and adjusted to produce balanced lateral soil displacements by having the rear gang extend wider than the front gang (Fig. 3b) and to have tapered disk blades (Fig. 3c) so that the field remains leveled, minimizing the formation of dead furrows and back furrows. If soil is either translocated beyond the implement's width forming a line of deposition, or soil is moved away from the boundary, creating a dead furrow, significant edge effects may be created. In the model, the net outward translocation that contributes to the formation of tillage berms is represented by the parameter α_B (positive). The formation of dead furrows could be modeled in a similar manner, using a negative α_B.

At Holly Springs, tillage was conducted at about 7 km/h close to the grass hedge, and soil was thrown into the vegetation due to the action of the forward gang of disks. The 4.1 m wide implement had gangs with nine disks, all 56 cm in diameter. The rear gang extended 23 cm to each side, beyond the front gang. In contrast, the 3.5 m wide disk used at Coffeeville had eight disks in the front gang and nine in the rear. Disks were 50 cm in diameter, with smaller disks (45 and 40 cm) fitted at the extremities of the rear gangs, which extended 86 cm wider to each side than the front gangs. At Coffeeville, tillage near the hedges was conducted at reduced speed to minimize the throwing of soil into the vegetation.

The differences in the implements used in the two fields explain the differences in edge-of-field berm expression at the two sites. The wider rear gang, tapered rear gang blades, and slower speed of operation resulted in no berm formation at Coffeeville; while the full-speed operation of the tandem disk with less rear gang offset allowed berms to quickly develop at Holly Springs. The position of the first pass near the edge of field is consistently maintained through the years at Holly springs due to the presence of a concrete edge and specific instruction to the operator that tillage passes be performed very close to the vegetation. Full speed tillage and instructions to keep vegetation in check make it likely that the Holly Springs result is similar to how many vegetative buffers could be managed in production fields. At Coffeeville, variation in the positioning of tillage passes in the vicinity of the vegetation was evident from the multiple steps along the downslope boundary. Indeed, the width of the hedges increased considerably between 1993 and 2001 (Dabney et al., 1999), as operators avoided tilling up the vegetation.

7.3. Landscape benching

The Coffeeville application illustrates the process of formation of bench terraces initiated with the introduction of vegetative barriers and developed with help of repeated tillage. The model predicts the contribution of tillage translocation to observed benching, while field observations reflect the combined effects of tillage and water erosion and deposition. The model can be used to provide a conservative estimate of how the landscape will change until a desired slope is achieved, or to determine when excessive benching may expose subsoil that will eventually lead to decreased

productivity. Dabney et al. (1999) used the Revised Universal Soil Loss Equation (RUSLE) to estimate soil erosion by water and concluded that annual average water erosion and tillage erosion were of similar magnitudes at this site. Comparison of measured and computed profiles in this study showed that the importance of water erosion/deposition was greatest where the field was crossed by a swale. The creation of deeper tractor wheel tracks and deeper tillage in this frequently wet zone could also account for the localized erosion in the proximity of the hedges

8. Conclusion

The implementation of specialized boundary conditions into the two-dimensional, grid-based tillage erosion model allowed its application to situations where internal boundaries determine the patterns of soil erosion and deposition within fields. The present work showed that a variety of situations commonly found in practice can be simulated with a few types of boundary conditions and how a specially designed boundary condition treatment allowed the modeling of formation of tillage berms.

Capturing the influence of field boundaries on tillage erosion is important because the morphological changes may be significant, especially when the field is partitioned by features such as fences or vegetative buffers. Depending on implement adjustment, edge-of-field berms may develop that are of a size that can significantly affect flow paths of runoff water. The difference in berm expression between the Holly Springs and Coffeeville locations emphasizes the need for additional research to quantify the α_B parameters of tillage implements.

The application of TELEM to the Coffeeville field demonstrates that the model can predict decadal tillage-induced topographic changes in actual fields with internal boundaries of complex shapes. These internal boundaries determine erosion patterns, and the resulting landscape evolution is of sufficient magnitude that future erosion rates due to both water and tillage will be significantly affected by the reduction in slope steepness resulting from landscape benching.

References

Bell, M., 1992. The prehistory of soil erosion. In: Bell, M., Boardman, J. (Eds.), Past and Present Soil Erosion: Archaeological and Geographical Perspectives, Oxbow Monograph 22. Oxbow Books, Oxford, UK, pp. 21–35.

Da Silva, J.R.J., Soares, J.M.C.N., Karlen, D.L., 2004. Implement and soil condition effects on tillage-induced erosion. Soil Tillage Res. 78, 207–216.

Dabney, S.M., 2006. Tillage erosion: terrace relationships. In: Lal, R. (Ed.), Encyclopedia of Soil Science. Marcel Dekker, New York, pp. 1752–1754.

Dabney, S.M., McGregor, K.C., Meyer, L.D., Grissinger, E.H., Foster, G.R., 1993. Vegetative barriers for runoff and sediment control. In: Mitchell, J.K. (Ed.), Integrated Resources Management and Landscape Modification for Environmental Protection. ASAE, St. Joseph, MI, pp. 60–70.

Dabney, S.M., Liu, Z., Lane, M., Douglas, J., Zhu, J., Flanagan, D.C., 1999. Landscape benching from tillage erosion between grass hedges. Soil Tillage Res. 51, 219–231.

De Alba, S., 2003. Simulating long-term soil redistribution generated by different patterns of mouldboard ploughing in landscapes of complex topography. Soil Tillage Res. 71, 71–86.

Dercon, G., Govers, G., Poesen, J., Sánchez, H., Rombaut, K., Vandenbroeck, E., Loaiza, G., Deckers, J., 2007. Animal-powered tillage erosion assessment in the southern Andes region of Ecuador. Geomorphology 87, 4–15.

Fowler, P.J., Evans, J.G., 1967. Plough-marks, lynchets and early fields. Antiquity 41, 289–301.

Govers, G., Quine, T.A., Desmet, P.J.J., Walling, D.E., 1996. The relative contribution of soil tillage and overland flow erosion to soil redistribution on agricultural land. Earth Surf. Processes Landforms 21, 929–946.

Heckrath, G., Halekoh, U., Djurhuus, J., Govers, G., 2006. The effect of tillage direction on soil redistribution by mouldboard ploughing on complex slopes. Soil Tillage Res. 88, 225–241.

Jacobson, P., 1963. New methods of bench terracing steep slopes. In: Transactions of the ASAE, Paper No. 62-716A, Winter Meeting of the ASAE, Chicago, pp. 257–261.

Lewis, L.A., 1992. Terracing and accelerated soil loss on Rwandian steeplands: a preliminary investigation of the implications of human activities affecting soil movement. Land Degrad. Rehab. 3, 241–246.

Li, S., Lobb, D.A., Lindstrom, M.J., Farenhorst, A., 2007a. Tillage and water erosion on different landscapes in the northern North American Great Plains evaluated using ^{137}Cs technique and soil erosion models. Catena 70, 493–505.

Li, S., Lobb, D.A., Lindstrom, M.J., 2007b. Tillage translocation and tillage erosion in cereal-based production in Manitoba, Canada. Soil Tillage Res. 94, 164–182.

Li, S., Lobb, D.A., Tiessen, K.H.D., 2009. Modeling tillage-induced morphological features in cultivated landscapes. Soil Tillage Res. 103, 33–45.

Lindstrom, M.J., Nelson, W.W., Schumacher, T.E., Lemme, G.D., 1990. Soil movement by tillage as affected by slope. Soil Tillage Res. 17, 255–264.

Lindstrom, M.J., Nelson, W.W., Schumacher, T.E., 1992. Quantifying tillage erosion rates due to moldboard plowing. Soil Tillage Res. 24, 243–255.

Lindstrom, M.J., Schumacher, J.A., Schumacher, T.E., 2000. TEP: a tillage erosion prediction model to calculate soil translocation rates from tillage. J. Soil Water Conserv. 55, 105–108.

Lobb, D.A., Kachanoski, R.G., 1999. Modelling tillage erosion in the topographically complex landscapes of southwestern Ontario, Canada. Soil Tillage Res. 51, 261–277.

Lobb, D.A., Kachanoski, R.G., Miller, M.H., 1995. Tillage translocation and tillage erosion of shoulder slope landscape positions measured using ^{137}Cs as a tracer. Can. J. Soil Sci. 75, 211–218.

Lobb, D.A., Kachanoski, R.G., Miller, M.H., 1999. Tillage translocation and tillage erosion in the complex upland landscapes of southwestern Ontario, Canada. Soil Tillage Res. 51, 189–209.

Lowdermilk, W.C., 1953. Conquest of the land through 7000 years. USDA Soil Conservation Service. Bulletin No. 99, Washington, DC, 30pp.

Nash, J.E., Sutcliffe, J.V., 1970. River flow forecasting through conceptual models. Part I – A discussion of principles. J. Hydrol. 10, 282–290.

Mutchler, C.K., McGregor, K.C., Cullum, R.F., 1994. Soil loss from contoured ridge-till. Trans. ASAE 37, 139–142.

Papendick, R.I., Miller, D.E., 1977. Conservation tillage in the Pacific Northwest. J. Soil Water Conserv. 32, 49–52.

Schumacher, T.E., Lindstrom, M.J., Schumacher, J.A., Lemme, G.D., 1999. Modeling spatial variation in productivity due to tillage and water erosion. Soil Tillage Res. 51, 331–339.

Smith, R.T., 1975. Early agriculture and soil degradation. In: Evans, J.G., Limbrey, S., Cleere, H. (Eds.), The Effect of Man on the Landscape: The Highland Zone. CBA Research Report. pp. 27–37.

Tiessen, K.H.D., Mehuys, G.R., Lobb, D.A., Rees, H.W., 2007a. Tillage erosion within potato production systems in Atlantic Canada. I. Measurement of tillage translocation by implements used in seedbed preparation. Soil Tillage Res. 95, 308–319.

Tiessen, K.H.D., Lobb, D.A., Mehuys, G.R., Rees, H.W., 2007b. Tillage erosion within potato production in Atlantic Canada: II. Erosivity of primary and secondary tillage operations. Soil Tillage Res. 95, 320–331.

Tiessen, K.H.D., Lobb, D.A., Mehuys, G.R., Rees, H.W., 2007c. Tillage translocation and tillage erosivity by planting, hilling and harvesting operations common to potato production in Atlantic Canada. Soil Tillage Res. 97, 123–139.

Tiessen, K.H.D., Li, S., Lobb, D.A., Mehuys, G.R., Rees, H.W., Chow, T.L., 2009. Using repeated measurements of 137cs and modelling to identify spatial patterns of tillage and water erosion within potato production in Atlantic Canada. Geoderma 153, 104–118.

Turkelboom, F., Poesen, J., Ohler, I., Ongprasert, S., 1999. Reassessment of tillage erosion rates by manual tillage on steep slopes in northern Thailand. Soil Tillage Res. 51, 245–259.

USDA-NRCS, 2003. Vegetative Barrier, Code 601. ftp://ftp-fc.sc.egov.usda.gov/NHQ/practice-standards/standards/601.pdf (accessed 28.09.09).

USDA-NRCS, 2007. Contour Buffer Strips, Code 332. ftp://ftp-fc.sc.egov.usda.gov/NHQ/practice-standards/standards/322.pdf (accessed 28.09.09).

Van Muysen, W., Govers, G., 2002. Soil displacement and tillage erosion during secondary tillage operations: the case of rotary harrow and seeding equipment. Soil Tillage Res. 65, 185–191.

Van Muysen, W., Govers, G., Van Oost, K., Van Rompaey, A., 2000. The effect of tillage depth, tillage speed, and soil condition on chisel tillage erosivity. J. Soil Water Conserv. 55, 355–364.

Van Muysen, W., Govers, G., Van Oost, K., 2002. Identification of important factors in the process of tillage erosion: the case of mouldboard tillage. Soil Tillage Res. 65, 77–93.

Van Muysen, W., Van Oost, K., Govers, G., 2006. Soil translocation resulting from multiple passes of tillage under normal field operating conditions. Soil Tillage Res. 87, 218–230.

Van Oost, K., Govers, G., Desmet, P., 2000. Evaluating the effects of changes in landscape structure on soil erosion by water and tillage. Landscape Ecol. 15, 577–589.

Vieira, D.A.N., Dabney, S.M., 2009. Modeling landscape evolution due to tillage: model development. Trans. ASABE 52, 1505–1522.